The FLUOR interferometric beam combiner
L'instrument interférométrique FLUOR

Vincent Coudé du Foresto[1], Gilles Chagnon[1], Marc Lacasse[2], Bertrand Mennesson[1], Sébastien Morel[1], Guy Perrin[1], Steve Ridgway[3], and Wesley Traub[2]

[1] Observatoire de Paris, DESPA, F-92195 Meudon Cedex, France
[2] Harvard-Smithsonian Center for Astrophysices, Cambridge MA 02138, USA
[3] National Optical Astronomy Observatories, Tucson AZ 85726, USA

Abstract. FLUOR stands for Fibered Linked Unit for Optical Recombination and is an interferometric instrument which started out as a technology demonstrator, demonstrated the potential of single-mode fiber optics for high precision visibility measurements, and has been operated as a focal instrument of the IOTA interferometer since 1995. After a presentation of the instrument, the programs carried out with FLUOR are reviewed, as well as the perspectives introduced by interferometric observations with a high dynamic range.

Keywords: Interferometry – Aperture Synthesis – High Angular Resolution – Guided optics – Stellar astrophysics

Résumé. FLUOR (Fiber Linked Unit for Optical Recombination) était conçu à l'origine comme un prototype destiné à démontrer l'intérêt du filtrage spatial de la turbulence atmosphérique pour améliorer la qualité des mesures de visibilités. Il a ensuite évolué pour devenir un véritable instrument focal de l'interféromètre IOTA, où il est utilisé par plusieurs groupes depuis 1995 pour des observations interférométriques en bande K (et plus récemment en bande L) de sources stellaires, obtenant de manière routinière des précisions meilleures que le pourcent sur les mesures de visibilité. Après une présentation de l'instrument, les programmes réalisés avec FLUOR seront passés en revue, ainsi que les perspectives apportées par l'observation interférométrique à grande dynamique.

Mots-clef : Interférométrie – Synthèse d'Ouverture – Haute Résolution Angulaire – Optique Guidée – Astrophysique Stellaire

1 Introduction

It was early realized [10] that single mode waveguides had an interesting potential for stellar long baseline interferometry: a single optical fiber can transport light through long and complicated paths without multiple reflections and diffraction effects, while still maintaining coherence information. Other optical functions needed for stellar interferometry (optical delay, beam

combination, polarization control...) can also be performed with fibered or integrated single-mode waveguides [13,27].

More importantly, single-mode fibers force the tranverse structure of the guided beam and therefore provide a perfect spatial filter to clean out the wavefront inhomogeneities caused by the atmospheric turbulence across each individual pupil. From the focal image at each telescope, only the coherent energy is extracted by the fiber and presented for beam combination. Therefore the random loss of coherence induced by turbulence, which is usually difficult to calibrate in multimode interferometers, is transformed into a random loss of intensity through the fiber, which can easily be monitored in order to derive visibility estimators insensitive to the spatial modes of turbulence.

This filtering property, however, comes at a cost, since photons are necessarily rejected in the process. The fraction of the energy coupled into the fiber is directly linked to the Strehl ratio [8], which in high turbulence conditions ($D \gg r0$, where D is the telescope diameter and r_0 Fried's parameter) is in average equal to the inverse $(r_0/D)^2$ of the number of speckles in the stellar image.

This implies that the amount of energy that can be coupled into the fiber from an uncompensated pupil is limited by the area πr_0^2 of a coherent cell in the atmospheric turbulence, which scales as $\lambda^{6/5}$. The longer the wavelength, the more light can be coupled into the fiber.

Silica glass single-mode fibers and couplers produced for the telecommunication industry have been around since the early 80's, and their application to stellar interferometry has been studied ever since [27,29,30]. Because they do not transmit much beyond $1.9\,\mu$m, their sensitivity is limited by the need to observe at visible or near-infrared wavelengths and so far their use on the sky has remained experimental.

In 1988, the MRT and CNES (French Ministery for Research and Technology, and space agency) co-funded a research and development program by Le Verre Fluoré company to provide single mode components made of fluoride glass (in partnership with Paris Observatory for the testing and validation of these components for astronomical use), whose good mid-infrared transmission enables observations through the atmospheric K band ($\lambda = 2.0 - 2.4\,\mu$m) and L band ($\lambda = 3.4 - 4.0\,\mu$m) windows. Apart from being less affected by atmospheric turbulence, these windows, which host important molecular lines (CO, NH3, H20...), are very interesting for the study of dust and gas diffusion processes in circumstellar environments, the possibility they offer to image embedded objects and to reduce the contrast between a star and a cool companion.

On the technological side, an attractive feature of fluoride glass is its lesser sensitivity to external perturbutions which reduces the need for most active controls found in silica fiber systems.

2 The Kitt Peak experiments

The first K band single-mode fiber drawn featured a 6.5 μm core within a 125 μm cladding, and a cutoff wavelength of 1.95 μm. It was used to manufacture X couplers which, by bringing the fiber cores close together, mix the evanescent waves in the cladding and act like the waveguide equivalent of a beamsplitter.

Three fiber couplers, spliced into a single triple coupler, formed the core of the first implementation of FLUOR [3], a fiber link between two independent 0.8 m telescopes on the McMath solar tower at Kitt Peak observatory in Arizona, transforming the pair into a stellar interferometer with a 5.5 m baseline. The triple coupler operated in the K band and had two inputs (one for each telescopes) and four outputs (Fig. 1): the two complementary interferometric outputs (I_1 and I_2), and two photometric outputs (P_1 and P_2) used to monitor the coupling fluctuations at each input. Altogether, the total length of fiber travelled by a photon was of the order of 3 m.

A simple example, using a monochromatic source at wave number σ, can show how fiber interferograms are corrected from the turbulence induced coupling fluctuations. Neglecting various transmission and proportionality factors, the expression of a generic raw interferogram I is (Fig. 2):

$$I(x) = P_1(x) + P_2(x) + 2\sqrt{P_1(x)\,P_2(x)}\;\mu\,\cos(2\pi\sigma x + \Phi), \tag{1}$$

where μ is the modulus of the complex coherence factor, x the optical path difference, and Φ a phase term. From this and with the knowledge of P_1 and P_2, it is easy to build the corrected interferogram (Fig. 3) whose modulated part is:

$$\begin{aligned} I_{\rm cor}(x) &= \frac{I(x) - P_1(x) - P_2(x)}{2\sqrt{P_1(x)\,P_2(x)}} \\ &= \mu\,\cos(2\pi\sigma x + \Phi). \end{aligned} \tag{2}$$

The quantity $1 + I_{\rm cor}$ is the normalized interferogram that would have been observed if there had been no atmospheric turbulence, i.e. if P_1 and P_2 had been equal and constant. From $I_{\rm cor}$ can be derived a fringe visibility measurement that does not depend on the loss of transverse coherence induced by the atmospheric turbulence on the pupil.

The first version of FLUOR was essentially a low-cost technology demonstrator, not optimized in many ways. Its aim was to demonstrate the interferometric combination of stellar beams using single-mode waveguides, and to validate the potential of spatial filtering for visibility calibration. The telescopes were 30 years old and not designed with interferometry in mind. The beams that fed the triple coupler, carried out to the recombination laboratory in a classical way by means of mirrors, were not stabilized and the tip-tilt phase errors were large. The triple coupler, not dispersion compensated, laid

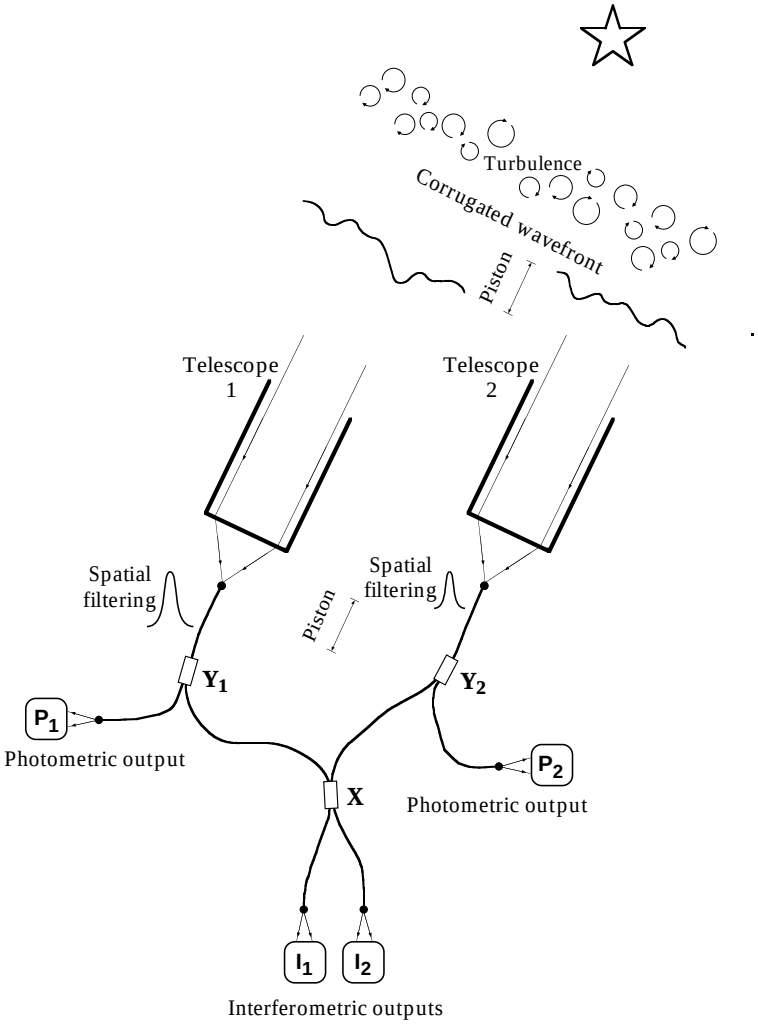

Fig. 1. Principle of the triple fiber coupler, with its two complementary interferometric outputs, and the photometric monitoring of coupling fluctuations at each telescope.

Fig. 3. The interferogram of Fig. 2, after correction.

unprotected on the optical bench and polarization control was rudimentary. Fringes were observed "on the fly" with a delay line that remained static during the observations, and the optical path difference was scanned at a rate set by the sideral motion (a typical fringe frequency was 320 μm/s for that east-west baseline). Signal detection was achieved by a set of four InSb fast photometers and a digitizing desktop computer. Despite the relatively crude apparatus, fringes were observed the first night the system was put into service, and calibrated visibilities were determined within 1–2 % [4], enough to measure a few diameters of supergiants, albeit with a fairly low productivity.

A second, more ambitious version of FLUOR was subsequently installed on the Kitt Peak site. It aimed at linking two telescopes (0.4 and 0.9 m) 53 m apart on an East–West baseline. It differed from the original version by the

longer baseline, the splitting of the triple coupler into three connectorized couplers for more flexibility, and the beam transport from the telescopes foci to the combination lab via a pair of 80 m long fibers. The optical delay was generated in the air between the fibers and the triple coupler.

That new implementation failed to produce stellar fringes but turned out to be much more instructive than the original version about a few key issues concerning single-mode fluoride waveguides:

- *Polarization control* Bends and twists in standard fibers introduce random birefringence and polarization dispersion which must be neutralized using dispersion compensators. An alternative solution consists in using polarization preserving fibers, whose anisotropic core provide well-defined slow and fast axes, with negligible crosstalk, and to treat each polarization separately in the interferometer [27].
- *Dispersion* FLUOR's visibility estimator [6], integrating the power spectral density of the fringes in the Fourier transform of the interferogram is, to a first order, insensitive to chromatic dispersion, which affects only the phase of the Fourier transform. However, a large excess of dispersion requires a longer scan, therefore adding noise. Because of waveguide inhomogeneities, such large amounts can be generated over tens of meters even if the fiber lengths are equalized. Differential dispersion can (and should) be compensated in the guided optics train, by measuring the phase curvature of a laboratory interferogram [5].
- *Connectorization* Efficient connectorization is important for a flexible rearrangement of waveguide components. Since the core of single-mode fluoride fibers is only a few microns in diameter, it should be positioned with a sub-micronic accuracy. The fluoride fiber core, however, is not necessarily concentric to its cladding, and therefore the connectors should provide the capability to dynamically center the fiber core with respect to the ferule. Cleanliness is also a paramount issue since a micron-sized particle deposited on the fiber core or the connector ferule may have dramatic consequences on the fiber-to-fiber coupling efficiency;
- *Others* Another important element of success for a stellar interferometer is the clear separation between the service functions (light collection, beam transportation, stabilization and delay) and the beam combining instrumentation. Besides, the sensitivity to correlated flux (the object's intensity times its visibility) should be adjusted with the baseline, as for a given source longer baselines provide lower correlated flux.

3 FLUOR on IOTA

Following the confidence built upon the success of the first FLUOR prototype and the lessons learned from the second Kitt Peak experiment, the latest version of FLUOR is now installed as a focal instrument at the IOTA (Infrared and Optical Telescope Array) interferometer, a L-shaped array located on

Mt Hopkins in Arizona and providing a number baselines ranging from 7 to 38 m in length and with different orientations [1]. In IOTA the beams are collected by 0.45 m siderostats, compressed ten times by afocal telescopes, stabilized by active tip-tilt correction, and transported and delayed by plane mirrors in a vacuum pipe up to the combination laboratory, where a dichroic beamsplitter separates the visible light (used by the tip-tilt sensor) from the infrared radiation. In the K band, and for typical seeing conditions on Mt Hopkins, $D \simeq r_0$ and most of the turbulent energy is in the (removed) tilt modes. Therefore FLUOR, as a focal instrument, receives in input a pair of 45 mm infrared beams, with moderate wavefront perturbations and zero geometrical delay (only remains the random delay introduced by the differential piston mode between the two pupils).

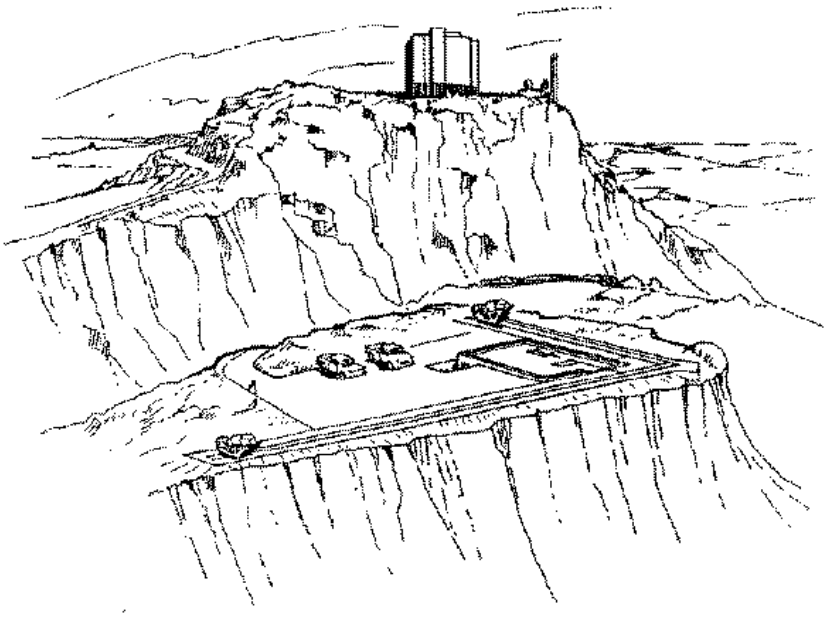

Fig. 4. Artist's view of the IOTA interferometer

FLUOR's layout on IOTA is very similar to the Kitt Peak experiment; a complete description of the setup (Fig. 5) can be found in [7,21,28]. The major modifications with respect to the Kitt Peak versions are:

- Improved detector: the four InSb single-pixels photometers are replaced by a single NICMOS array, resulting in a 100x sensitivity gain for a new limit magnitude $K \simeq 5$. Only four pixels of the array are read, at a fast (1–2 kHz) rate: on these pixels are imaged the four output fiber heads

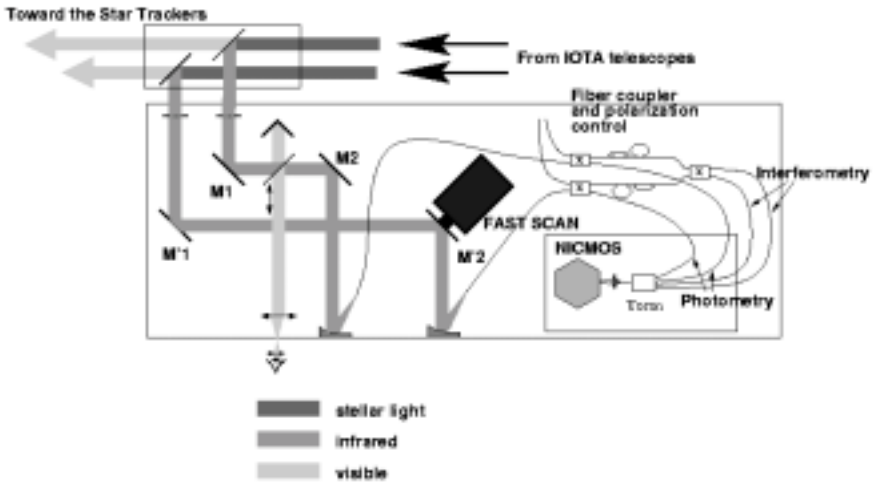

Fig. 5. Optical layout of the FLUOR table at IOTA.

(arranged in a single bundle with claddings side by side so that the cores form a 125 μm square);

- Waveguide protection and connectorization: The triple coupler and polarization controllers are inserted inside a box (Fig. 6) for passive protection against external perturbations. Newer technology connectors (series E2000 from Diamond) with dynamic centering of the fiber core enable a good throughput from the triple coupler to the output fiber bundle;
- Optical pathlength modulation and control: fringes packets are obtained by repetitive scans (with a piezo mounted mirror) through the zero optical delay point. Up to 2 scans per second can be performed, while the fringe modulation rate (typically 100 to 500 Hz) is a compromise between the need to freeze the atmospheric piston and the need to minimize detector readout noise. Because of the atmospheric piston also, the fringe packet is not centered in the scan. The offset of the fringe packet center is fed back into IOTA's delay line to ensure that the zero path difference is tracked in close loop, albeit at a rate slower than the coherence time of the atmosphere (coherencing);

FLUOR data are quite strongly structured. Fringe packets are acquired by batches of 100 to 500 scans on-source, representing a few minutes of observation (Fig. 7). Each batch needs to be complemented by the acquisition of a smaller batch off-source, as well as batches with only one of the two beams feeding the triple coupler. These four batches, together with ancillary information, form an observation block, the smallest self-consistent set of data which enables the determination of a squared raw visibility (μ^2) on a single source. The object visibility (V^2) is linked to the raw visibility via the instrument's point source response or transfer function (T^2): $\mu^2 = T^2V^2$, which

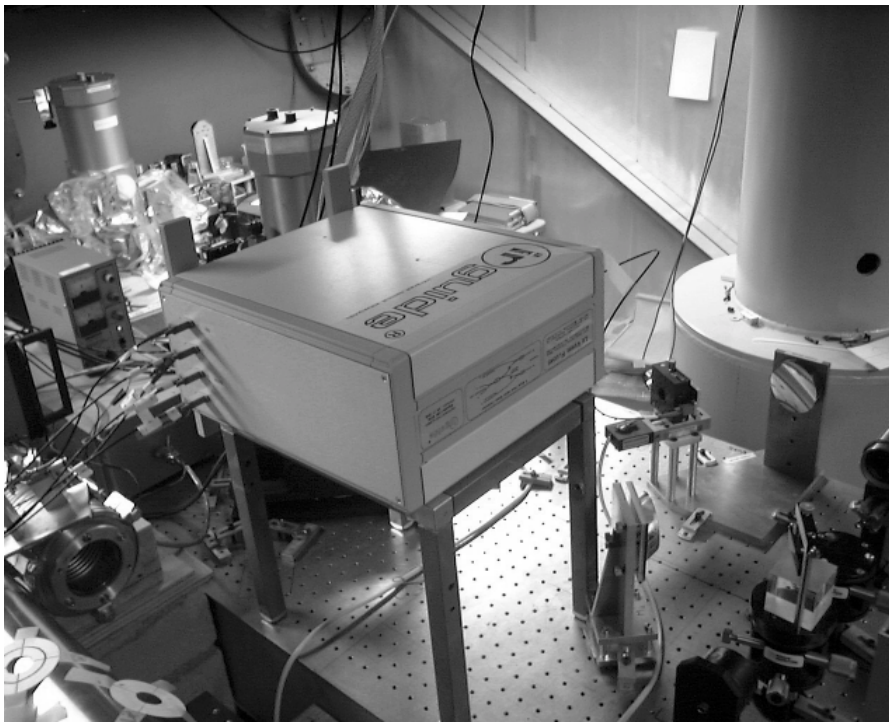

Fig. 6. The optical correlator box on the FLUOR table. The four output fiber connectors can be seen on the left side.

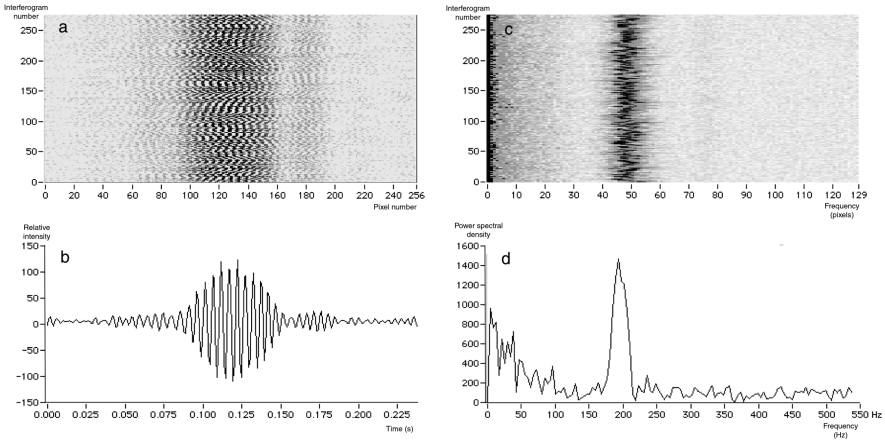

Fig. 7. An example of raw FLUOR data: (a) waterfall display of a batch of 275 interferograms (after recentering by the coherencing algorithm) and (b) a single filtered time sequence; (c) waterfall display of the power spectra and (d) a single full power spectrum, containing the fringe signal and the low frequency signature of the photometric fluctuations.

evolves over a few percents during the night and needs to be calibrated regularly by observing a reference source for which the object visibility is known *a priori*. A chain of observation blocks obtained alternately on reference sources and science targets forms an observation file, the smallest data entity that can provide calibrated object visibilities. During a good night about $\simeq 40$ observation blocks can be acquired, yielding about half as many calibrated visibilities on science targets.

Transforming FLUOR from a prototype to a productive scientific instrument required the development of a substantial amount of supportive software for the preparation of observations (determination of expected visibilities and optimization of observation scenarii to minimize delay line repositioning), data acquisition, data quality assessment, pipeline data reduction (from observation files of raw data to calibrated visibilities with their error bars), and archiving.

To ensure proper calibration, a catalog of reliable reference sources is also an important part of the instrument: it is based on the work of [2] which provides a grid of 422 photometric calibrators (one every 10 degrees on the sky in average), whose diameters can be predicted within 1–2 %. This is sufficient to ensure that the uncertainty on the reference diameter almost always accounts for a negligeable amount in the error bar on the transfer function.

Calibrated visibilities and their formal error bars are derived from the interpolation of the transfer function and the statistical errors on raw visibilities, as detailed in [22]. Statistical errors can be dominated either by an additive detector noise (for the faintest sources), stellar shot noise or the multiplicative piston noise of the atmosphere, the zero-order turbulence mode which is not filtered out by the fiber. For the brightest sources with high visibility the detection noises are negligeable and the relative precision $\delta V/V$ of the calibrated visibilities can reach 0.3 %.

4 Thermal infrared extension

Since 1998, FLUOR can also be operated at longer wavelengths, in the 3.4–4.0 μm L band, using a dedicated X-coupler [18,19]. IOTA/FLUOR is the first and, to date, the only interferometer that can observe in L. The thermal infrared is characterized by specific constraints with respect to the K band: the seeing is better with a lower d/r_0 ratio and longer coherence time, but the interferometric signal is contaminated by an incoherent thermal background which needs to be minimized, monitored, and properly substracted in order to achieve high accuracy visibility measurements. Because the NICMOS camera is not sensitive beyond 2.5 μm, the noisier InSb photometers have to be used, resulting in a limit magnitude of $L \simeq -1$.

5 Science programs

The FLUOR/IOTA combination is well suited to observe at very high angular resolution (with a 38 m baseline $\lambda/B = 12$ mas and 20 mas in the K and L bands, respectively) relatively bright ($K < 5$ or $L < -1$) and compact sources, since the field of view of a single-mode instrument is limited by the diffraction of a single subpupil (1 arcsec in K or 1.7 arcsec in L). This is well suited to study classes of sources which include stellar photospheres (most notably late type giants), circumstellar environments, and close binaries.

As is the case with a two telescope interferometer, no direct image is produced but instead visibility amplitudes are measured for different spatial frequencies, which are then used to constrain models on the morphology of the source. The simplest model one can think of for a star is a uniform disk; a single visibility point is then sufficient to determine its diameter, while more points help confirm the validity of the uniform disk approximation and refine the measurement. Combined with bolometric fluxes, diameters yield photospheric effective temperatures, which are useful as benchmarks in evaluating models of stellar atmospheres. A campaign on giant cool stars has confirmed the previously known calibration of the temperature scale from M0 to M5, and extended it to spectral types M6 to M8 [22].

Many late-type giants are unstable, however, and undergo strong pulsations. Among them, the Mira type variables are also characterized by a very strong mass loss (10^{-5} to $10^{-4} M_\odot$/year) whose underlying physical mechanism is not yet fully understood, and the material shed out forms an envelope around the star. Mira variables have been particularly monitored with FLUOR [12,23]. Effective temperatures and mean linear radii show that (at least in the case of R Leo and R Aql) the pulsation occurs along the fundamental mode. While morphological changes during a cycle are readily apparent (Fig. 8), the visibility curve, very different from that of a uniform disk, also disagrees with the luminosity profiles predicted by current model atmospheres. In the L band the surrounding envelope dominates which makes the source appear larger, a phenomenon that is barely seen with heterodyne interferometry at 11 μm. Diffusion models which explain this behavior still have to be developed, while narrow band observations in CO, H_2O molecular lines and the nearby continuum should help provide a clearer picture.

Another highly interesting class of pulsating supergiants is the Cepheids which are, thanks to their period–luminosity relationship, the primary distance indicators for extragalactic astronomy. By monitoring the pulsation amplitude, interferometry can help calibrate the relationship independently of atmosphere models. Cepheids are a challenging target for interferometers like IOTA, because even the brightest ones are far away and barely resolved. But with the high visibility accuracy provided by FLUOR, it is possible to determine angular diameters much smaller than the diffraction limit λ/B: for example, the mean angular diameter of ζ Gem was found to be 1.64 +0.14 -0.16 mas [15].

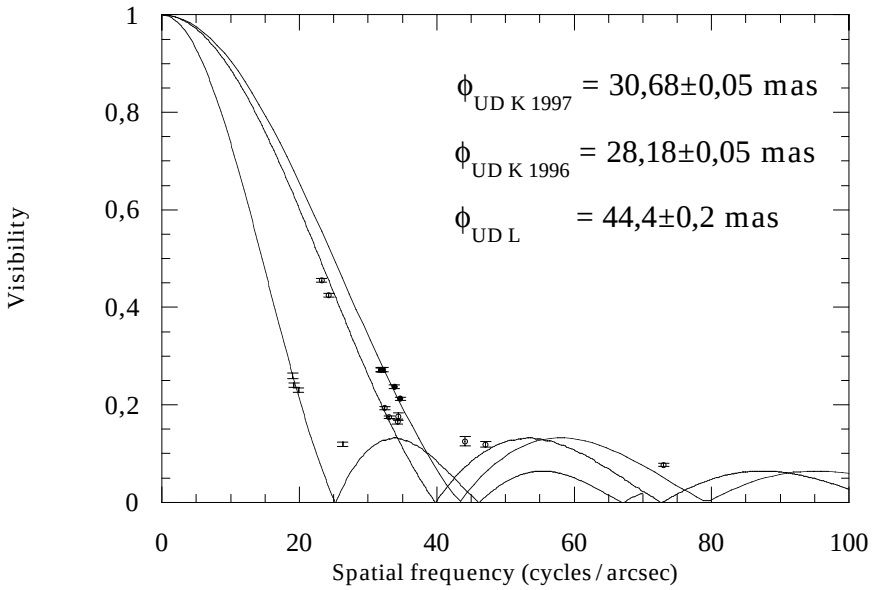

Fig. 8. Visibility curves of the Mira star R Leo showing the morphology changes in K between two different epochs (open and filled circles), and the increase in apparent size in the L band (vertical bars). The solid lines are the best fits by a uniform disk model, ϕ_{UD} the corresponding diameter.

Other ongoing programs include the study of irregular variables, asymetries and surface features in the atmosphere of supergiants, the search for binarity in λ Boo stars, and close binary observations, either as a follow-up of lunar occultations or radial velocity measurements.

6 Prospective

Future science programs on IOTA will further exploit the unique combination of high dynamic range and high angular resolution provided by FLUOR. It should be possible for example to constrain disk profiles around a handful of young stellar objects and B[e] stars, or to fully characterize spectroscopic binaries with low mass companions.

The next step will be to increase the resolution with longer baselines, and enhance the sensitivity with larger apertures (corrected by adaptive optics for efficient injection into the fibers) and fringe stabilization (to remove the piston perturbations). This will be achieved with the VLTI (ESO's Very Large Telescope Interferometer [11], which is being progressively implemented on the Paranal mountain in northern Chile. When completed, the VLTI main array will provide four 8 m telescopes with baselines of up to 120 m, while the sub-array includes at least three 1.8 m telescopes and a maximum baseline of

200 m. The two VLTI first-generation science instruments, AMBER [26] for the near infrared, and MIDI [25] for the thermal infrared beyond 8 μm, include fibered spatial filters and retain the principle of photometric calibration for ultimate visibility accuracy. The commissionning instrument, VINCI [14], is even a direct conceptual copy of FLUOR. The scientific potential of the VLTI is considerable: in its most sensitive mode it is not be limited to stellar physics, and will enable milliarcsecond observations of extragalactic sources such as quasars or active galactic nuclei.

Most of these sources have a luminosity distribution with a high dynamic range, requiring therefore high visibility accuracies, and a still open question is the ultimate performance that can be obtained with spatial filtering and photometric calibration. Currently the limit (0.3 %) for bright sources is set by the differential piston noise between the pupils. Random optical path-length difference fluctuations will ultimately be removed through servoed fringe tracking; what the limit then will be is unknown.

Using kilometric polarization preserving fibers balanced in dispersion, still wider arrays of large telescopes can be built: the 'Ohana project [17,24] aims at linking the major telescopes of the Mauna Kea observatory in Hawaii to achieve the same sensitivity as the VLTI main array but with a six-fold gain in baselines. The first interferometric connection is scheduled to be demonstrated in 2002. In a longer term, ALIRA is a proposed extension to the thermal infrared of the submillimetric ALMA array [9], using single-mode fibers currently in development that will be transparent in the 8–25 μm range.

Thermal infrared fibers may also play a key role in ESA's proposed DARWIN space exobiology mission, which aims at detecting Earth-type planets around nearby stars and characterizing their atmosphere [16]. In the current concept DARWIN blocks interferometrically the stellar light while allowing maximum transmission for the planet photons. To achieve a sufficient null, the residual phase requirements on the pupils are unrealistic unless spatial filtering is applied [20].

Finally, it is expected that in the future fibers will be used mostly for beam transportations, while most other optical functions will be integrated on optical chips [13]. This should considerably reduce the cost and complexity of interferometric instrumentation. Recently, the first stellar fringes with an integrated optics beam combiner (a triple coupler smaller than a stamp) have been obtained at the IOTA interferometer with the IONIC setup.

7 Conclusion

FLUOR's original purpose was to demonstrate high accuracy visibility measurements through spatial filtering and photometric calibration. These principles are now adopted by most stellar interferometers around the world. Then it was installed as a regular beam combiner at the IOTA interferometer, and in the last 5 years has produced a wealth of scientific data. The instrument

has reached a level of maturity which makes it possible for external groups, not involved in its development nor even very familiar with stellar interferometry, to efficiently carry out their own programs with it. In such, it also plays a training role to prepare the community to the VLTI and other next generation interferometers.

References

1. Carleton N.P., et al., 1994, in: Amplitude and Intensity Spatial Interferometry II. SPIE 2200, p. 152
2. Cohen M., et al., 1999, AJ 117, 1864
3. Coudé du Foresto V., Ridgway S., 1991, in: Beckers J., Merkle F. (eds.) High-resolution imaging by interferometry II. Garching, p. 731
4. Coudé du Foresto V., 1994, PhD thesis, Université Denis Diderot (Paris 7)
5. Coudé du Foresto V., et al., 1995, A&A 293, 278
6. Coudé du Foresto V., et al., 1997, A&AS 121, 379
7. Coudé du Foresto V., et al., 1998, SPIE 3350, p. 856
8. Coudé du Foresto V., et al., 2000, A&AS 145, 305
9. Coudé du Foresto V., et al., 2000, *Journées ALMA, Institut d'Astrophysique de Paris*
10. Froehly C., 1981, in: Ulrich M.H., Kjär K. (eds.) Scientific Importance of High Angular Resolution at Infrared and Optical Wavelengths. ESO, Garching, p. 285
11. Glindemann A., 2001, these proceedings
12. Hofmann K.H., et al., 2000, SPIE 4006, p. 688
13. Kern, P., et al., 2001, these proceedings
14. Kervella P., et al., 2000, SPIE 4006, p. 31
15. Kervella P., et al., 2000, A&A, in press
16. Lund, G., et al., 2001, these proceedings
17. Mariotti J.-M., et al., 1996, A&AS 116, 381
18. Mennesson B., et al., 1999, A&A 346, 181
19. Mennesson B., 1999, PhD thesis, Université Denis Diderot (Paris 7)
20. Ollivier M., Mariotti J.-M., 1997, Applied Optics 36, 5340
21. Perrin G., 1996, PhD thesis, Université Denis Diderot (Paris 7)
22. Perrin G., et al., 1998, A&A 331, 619
23. Perrin G., 1999, A&A 345, 221
24. Perrin G., et al., 2000, SPIE 4006, p. 708
25. Perrin, G., et al., 2001, these proceedings
26. Pétrov, R., et al., 2001, these proceedings
27. Reynaud F., et al., 2001, these proceedings
28. Ruilier C., 1999, PhD thesis, Université Denis Diderot (Paris 7)
29. Shaklan S., Roddier F., 1987, Applied Optics 26, 2159
30. Shaklan S., 1990, Optical Engineering 29, 684